

The influence of water on protein properties

Francesco Mallamace,^{1,2,3,4,a)} Piero Baglioni,⁵ Carmelo Corsaro,¹ Sow-Hsin Chen,² Domenico Mallamace,⁶ Cirino Vasi,⁴ and H. Eugene Stanley³

¹*Dipartimento di Fisica e Scienze della Terra, Università di Messina, I-98166, Messina, Italy*

²*Department of Nuclear Science and Engineering, Massachusetts Institute of Technology, Cambridge, Massachusetts 02139, USA*

³*Center for Polymer Studies and Department of Physics, Boston University, Boston, Massachusetts 02215, USA*

⁴*Consiglio Nazionale delle Ricerche-IPCF, I-98166, Messina, Italy*

⁵*Dipartimento di Chimica and CSGI, Università di Firenze, 50019 Firenze, Italy*

⁶*Dipartimento di Scienze dell'Ambiente, della Sicurezza, del Territorio, degli Alimenti e della Salute, Università di Messina Viale F. Stagno d'Alcontres 31, 98166 Messina, Italy*

(Received 9 September 2014; accepted 15 October 2014; published online 31 October 2014)

The “dynamic” or “glass” transition in biomolecules is as important to their functioning as the folding process. This transition occurs in the low temperature regime and has been related to the onset of biochemical activity that is dependent on the hydration level. This protein transition is believed to be triggered by the strong hydrogen bond coupling in the hydration water. We study the vibrational bending mode and measure it using Fourier Transform Infrared spectroscopy. We demonstrate that at the molecular level the hydration water bending mode bonds the C=O and N–H peptide groups, and find that the temperature of the “dynamic” protein transition is the same as the fragile-to-strong dynamic transition in confined water. The fragile-to-strong dynamic transition in water governs the nature of the H bonds between water and peptides and appears to be universal in supercooled glass-forming liquids. © 2014 AIP Publishing LLC. [<http://dx.doi.org/10.1063/1.4900500>]

I. INTRODUCTION

Although water is one of the simplest molecules, it has intriguing and counterintuitive behaviors that have not clearly been explained.¹ Water is essential for life and is important to the structure, stability, dynamics, and function of biological macromolecules. An example is the reversible protein folding-unfolding process in which water mediates the collapse of the chain and the search for the native topology through a funneled energy landscape. Another is the role played by water in the life of the cell. There are thus many reasons this liquid should not be treated as a solvent only, but rather as an integral and active component of biomolecular systems, i.e., it is itself “a biomolecule” with fundamental dynamic and structural roles.²

Water is a central research topic in physics, chemistry, and biology, and an enormous number of studies have been conducted to probe its unusual properties. The results have converged on the idea that hydrogen bond (HB) interactions between water molecules are the key to understanding water’s properties and functions, especially in biological environments.³ HB clustering explains such anomalies of water as the density maximum at 4 °C and, when the temperature is decreased into the supercooled region of the phase diagram, the diverging of various thermal response functions.¹ As T decreases the HBs cluster and form an open tetrahedrally-coordinated HB network. When the T of the stable liquid phase is lowered, both HB lifetime and cluster stability in-

crease, and this altered local structure can, in principle, continue down to the amorphous region of the phase diagram.

Below $T_g \approx 130$ K water is a glass. Above that temperature it becomes a highly viscous fluid that crystallizes at $T_X \approx 150$ K. Amorphous water, like ice, is polymorphic. The two phases of glassy amorphous water—Low Density Amorphous (LDA) and High Density Amorphous (HDA)—can be transformed from one to the other by tuning the pressure. Metastable supercooled water is located on the phase diagram between the homogeneous nucleation temperature $T_H = 231$ K and the melting temperature $T_M = 273$ K. Thus, the region between T_X and T_H is a “No-Man’s Land” within which bulk liquid water is not experimentally accessible.¹ However, crystallization can be retarded by confining water within narrow nanoporous structures.

The existence of polymorphic glassy water and the behavior of HB networking suggests that liquid water may be also polymorphous, a mixture of low-density liquid (LDL) and high-density liquid (HDL). In the HDL phase, predominating in the high T regime, the local tetrahedrally-coordinated HB structure is not fully developed, but in the LDL a more open “ice-like” HB network appears. Thus water’s anomalies are caused by the “competition” between these two local liquid forms. Recent studies of confined water^{4,5} clearly show that when T is decreased to a certain point the water HB lifetime increases by approximately six orders of magnitude, indicating, at ambient pressure, the presence of a dynamic crossover from a super-Arrhenius (fragile liquid) to an Arrhenius (strong liquid) at $T_L \approx 225$ K. At this temperature the Stokes-Einstein relation is violated^{4,6} and clear signs of LDL and HDL are observed,⁵ suggesting that polymorphism also exists in the liquid phase.

^{a)} Author to whom correspondence should be addressed. Electronic mail: francesco.mallamace@unime.it

This fragile-to-strong dynamic crossover (FSDC) can be considered as a phenomenon that characterizes not only water but all the supercooled glass-forming liquids.⁷ The FSDC, with $T_L > T_g$, has also been recognized to sign the way with which the system dynamic arrest is approached:⁷⁻¹⁷ a lot of special processes take place there, see, e.g., Ref. 10. We mention, together with the violation of the Stokes Einstein law, the orientational-translational decoupling (the translation-rotation paradox¹⁸), the splitting of the relaxation into the primary (α) and secondary relaxation times, the onset of dynamical heterogeneities and of the Boson peak (hypothesized for bulk water¹⁴ and observed in the confined one¹⁵). The FSDC appears to be of importance also for hydrated proteins; the phenomenon can be observed not only for confined water but also for hydrated biosystems such as proteins,^{17,19-24} where the Boson peak has been also observed.^{16,25} For clarity we note that, besides these many signatures on the FSDC importance in material science, it has been questioned especially in the case of the water-protein systems.^{26,27}

Recent approaches to estimating T_L have stressed the fundamental importance of the crossover across various subfields of material science. It has been proposed that the concept of FSDC must be of interest not only in determining how a system arrests its dynamics but also because it opens up new frontiers in material science by suggesting how the understanding mechanisms at the microscale allows predictions of functional behavior at the macroscale.⁸ This concept has been explained using the well-known potential energy landscape (or the inherent structures) and by taking into account the molecular configurations (configuration entropy).²⁸ In this framework, the fragile fast dynamics of supercooled liquids correspond to intrabasin motions and the strong slow dynamics to interbasin motions (hopping over barriers of uniform height). At the lowest T the multibasin dynamics, i.e., arrest behavior, is favored. In the case of water the HB clustering is predominant, and below T_L the only relevant dynamics is that of molecules hopping from one cluster to another, i.e., a process with only one typical energy scale—the Arrhenius. Note that the inherent structure approach is in many way analogous to the so-called kinetic hypothesis of folding (the folding funnel) in which the native protein structure corresponds to the deep and stable local energy minimum as a function of the possible configurations, and many conformational substates in a definite biomolecule conformation are possible.²⁹

In addition to the folding process, of central interest in biology, the “dynamic” transition that biomolecules undergo in the low- T regime has the same importance. At the lowest temperatures proteins exist in a glassy state, a solid-like structure without conformational flexibility.³⁰ When T is increased, the atomic motional amplitude, measured using mean-squared atomic displacement $\langle X^2 \rangle$ (MSD), increases linearly, as in a harmonic solid. The atomic motional amplitude rate in hydrated proteins suddenly increases at ~ 220 K, signaling the onset of an additional anharmonic and liquid-like motion.^{31,32} The functions and the kinetics of biochemical reactions of many proteins slow sharply at a temperature, T_C , in a universal interval 240–200 K.³³ This transition can be suppressed in dry biomolecules³² and is solvent dependent. The biochem-

ical activity in proteins depends on their level of hydration, h (i.e., grams of H_2O per grams of dry protein). In the case of lysozyme the hydration level $h = 0.3$ corresponds to a water monolayer covering the protein surface, and the enzymatic activity is very low up to a hydration level of 0.2 and then increases sharply with an increase in h from 0.2 to 0.5.³⁴

Besides the bulk water, water molecules in a protein solution belong to two categories: the bound internal water and the surface (or hydration) water. Both have important roles in determining the protein properties.³⁵ Hydration water is the first layer of water in strong interaction with the protein surface. The bound internal water molecules, located in internal cavities and clefts, are known to be extensively involved in the protein-solvent H-bonding and play a structural role in the folded protein itself. The hydration water, interacting with the solvent-exposed protein atoms of different chemical character, feels the topology and roughness of the protein surface, and is believed to have an important role in controlling the biofunctionality of the protein.^{36,37} Water can influence both the hydrophilic and hydrophobic side groups of a biomolecule. The hydrophilicity (the HB strength) is a force that governs the secondary structure and folding specificity in proteins,³⁸ but the properties of the biomolecule can also be affected by the protein methyl groups, which are a factor in the dynamic transition. It has been experimentally shown that although a single hydration water layer can influence both the hydrophilic chains and the dynamics of the whole protein, the dynamic effects on the methyl chains are minimal. Their motions are confined and attributed to librational and rotational movements. Several hydration shells of water are required for the hydrophobic side chains to exhibit, at room temperature, the full range of motions characteristic of a liquid-like protein state.³⁹ Hence, because the properties of the surface water (the first layer water network) are intimately connected to protein stability and function, hydrophilic interactions with peptide groups are the most important topic when studying biological systems.

The approximate coincidence of these two characteristic temperatures— T_L for the dynamic crossover in water and T_C for the slowing of biochemical activities—and the $\langle X^2 \rangle$ sharp rise in biomolecules, has suggested a connection between the two phenomena. Specifically, this “dynamic” transition in proteins is believed to be triggered by their strong hydrogen-bond coupling with the hydration water.⁴⁰ This behavior has been observed in several biomolecules, including globular proteins,^{19,20} DNA, and RNA.²¹

This dynamic crossover in protein water has been studied by measuring the MSD and the transport parameters—the self-diffusion coefficient D and the average translational relaxation time $\langle \tau \rangle$ as a function of T —using various experimental techniques ranging from neutron scattering¹⁹ to nuclear magnetic resonance (NMR).²² The MSD encompasses vibrations and librations of the hydrogen atoms with respect to their binding center in the molecules, as well as large amplitude transitions between conformational substates of the macromolecule. It is thus difficult to identify “local” microscopic processes underlying this transition by means of neutron scattering or to pinpoint the actual dynamic transition temperature from the $\langle X^2 \rangle$. Dynamic and transport quantities

have also shown a sharper transition as a function of temperature and pressure that is connected to a dynamic transition in the hydration water.^{19,22}

II. METHODS

A. Sample preparation and experimental set-up

In this work, we deal with dynamics in a powder of the globular protein lysozyme hydrated with a single monolayer of water. The sample was prepared according to a well precise procedure.¹⁹ The dried protein powder was hydrated isopiesticly at 5 °C by exposing it to water vapor in a closed chamber until the wanted hydration level h is reached (here we have worked at $h = 0.3$ and 0.37). Differential scanning calorimetry (DSC) was performed to test the absence of bulk-like water.

FTIR absorption measurements were performed at ambient pressure by using a Perkin Elmer Spectrum GX Fourier transform spectrometer in the attenuated total reflection (ATR) geometry. The spectra of interest were recorded with the resolution of 4 cm^{-1} , automatically adding 250 repetitive scans in order to obtain highly reproducible spectra; then they were properly normalized. Samples were initially cooled at 180 K and the measurements were performed by increasing T with steps of 10 K in the range 180–350 K, i.e., from below the protein dynamical crossover temperature in the protein native state to above the irreversible denaturation ($T_D \approx 345$ K). The temperature increase was slow and its stability was maintained in the range of 0.1 K.

B. The vibrational bending mode

Figure 1 reports the vibrational bending mode of the pure bulk water (upper panel) and the peptide modes falling in this bending spectral region ($1300 < \nu < 1800 \text{ cm}^{-1}$): amide I, amide II, and amide III (lower panel). The peptide groups are described in IR and Raman spectroscopy with 9 characteristic bands named amide A, B, and I–VII in order of decreasing frequency. Amide I and amide II are the two major bands of the protein infrared spectrum. The amide A ($\sim 3500 \text{ cm}^{-1}$) and B ($\sim 3100 \text{ cm}^{-1}$) are due to a Fermi resonance between the first overtone of amide II and the N–H stretching vibration. The amide I band is mainly associated with the C=O stretching vibration related to the protein backbone. The amide II results essentially from the N–H bending vibration and from the C–N stretching vibration, respectively, at 1540 and 1520 cm^{-1} . This latter stretching, conformationally sensitive, is related with the antiparallel β -sheet structure of peptides and proteins. Amide III and IV, resulting from a mixture of several coordinate displacements, are very complex. The out-of-plane motions are found in amide V, VI, and VII. The amide I, II, and III are, respectively, used to assign proteins secondary structure.⁴¹ As shown in Figure 1, all these latter three bands of the protein peptides fall just within the frequency range in which the water bending modes are located (1300–1800 cm^{-1}). Water has essentially two bending modes—one at $\sim 1560 \text{ cm}^{-1}$ caused by molecules clustered in the network (i.e., only the four-bonded or LDL), and one at $\sim 1640 \text{ cm}^{-1}$ that is sharper and represents the remaining,

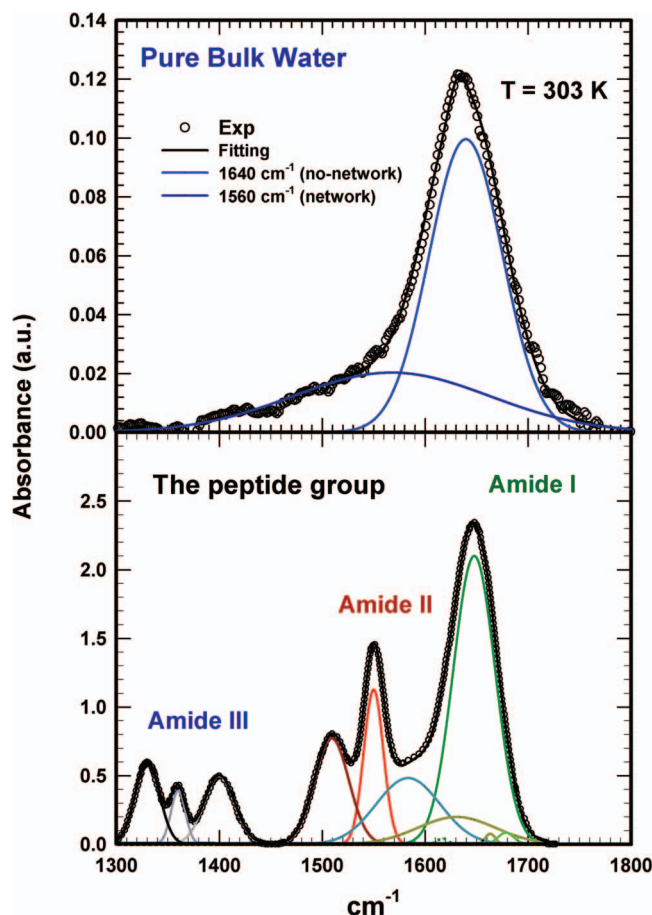


FIG. 1. The bending spectrum of pure bulk water at 303 K (top) in the range $1300 < \nu < 1800 \text{ cm}^{-1}$. The peptide groups (amide I, amide II, and amide III) falling in the same spectral range (bottom panel).

non-clustered free network molecules (HDL).⁴² The amide I absorption is primarily determined by the backbone conformation being independent of the amino acid sequence, its hydrophilic or hydrophobic properties and charge. Contribute to this band: the α -helix (1650 – 1657 cm^{-1}), the antiparallel β -sheets (two contributions in the ranges 1612–1640 cm^{-1} and 1680–1689 cm^{-1}) and the random coil near 1680 cm^{-1} . Well clear differences can be observed between the native and denatured protein states in agreement with literature data,⁴³ another process characterizing the denaturation (hence used to follow unfolding) is identified in the amide II band: the disappearance of the amide II N–H residual (1530–1550 cm^{-1}). Deuterated water can be used to study amide I and amide II bands, but the corresponding measured spectra are sensitive to the solvent. Furthermore, the spectrum may be more complicated for the isotopic exchange; for example, in the amide II, where much of its absorbance is due to N–H bending there is a large frequency shift upon H–D exchange. Analogous situation can be observed in the amide I band where its absorbance is due primarily to C=O stretching coupled to the N–H bending and C–H stretching modes.

The measured spectra are customary analyzed as a spectral deconvolution of Gaussian band shapes by an iterative curve fitting procedure and Figure 2 reports the obtained spectra in the water lysozyme system with a hydration level

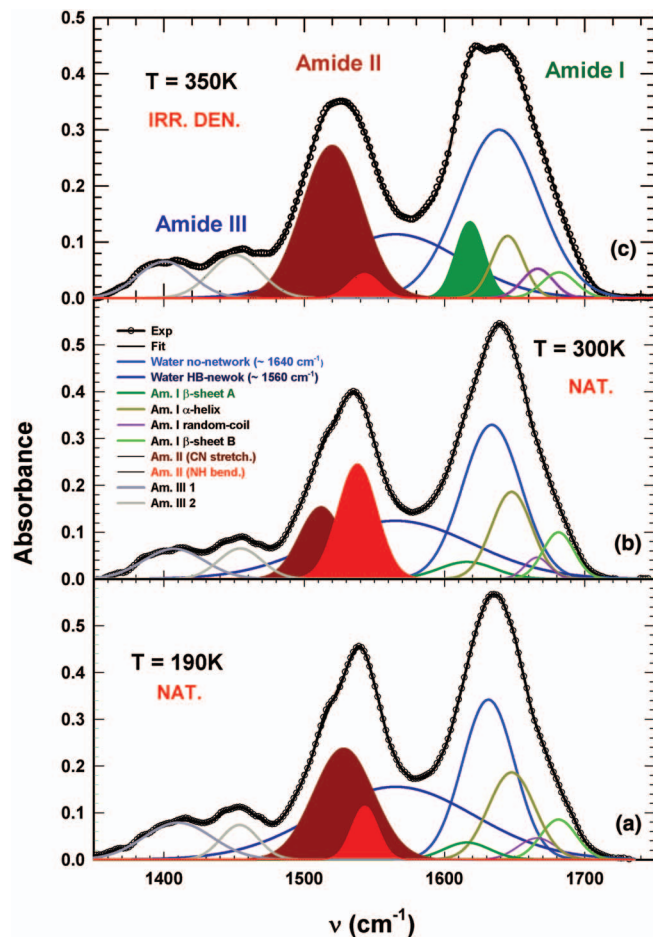


FIG. 2. The measured FTIR spectra in the water lysozyme system with the hydration level $h = 0.3$, at three different temperatures; respectively, in the native state below ($T = 190$ K (a)) and above ($T = 300$ K (b)) the protein dynamical crossover and finally in the irreversible denatured state ($T = 350$ K (c)). The figure shows the water and the peptide (amide I, II, and III) components.

of $h = 0.3$, at three different temperatures: in the native state below ($T = 190$ K, panel (a)) and above ($T = 300$ K, panel (b)) the protein dynamical crossover and in the irreversible denatured state ($T = 350$ K, panel (c)), the protein denatures at $T_D \approx 345$ K). The reported spectra have been studied by considering together with the amide contributions (I, II, and III) also those of water, namely, outside and inside the HB network, located at about 1640 and 1560 cm^{-1} , respectively (see top panel in Figure 1). Hence, our interest was focused on the amide I (C=O stretching in the protein backbone), the amide II (N–H bending and C–N stretching), and finally the two water components. The measured spectra appear to be very different not only in native and denatured states, but also in the native state above and below the crossover temperature. From these spectral fittings we have considered, at the studied temperatures, the integrated areas and the full width at half maximum (FWHM) of all the different Gaussian components. Due to the limited spectral resolution the variation of the frequency was not taken into account. We have considered the water contributions and amide II (N–H bending and C–N stretching) and the amide I (C=O vibration reflected in the two β -sheets contributions, the α -helix and the random coil). A visual inspection of Figure 2 evidences differences

in the two native phase spectra, in the absorbance intensity of the amide II and in the broadness of the amide I contributions. In the denatured phase the findings of a recent experiment on the unfolding of the same protein adsorbed in lipid bilayers are fully confirmed:⁴³ the nearly disappearance of the amide II N–H residual and the large increase of the antiparallel β -sheet contribution. This situation is accompanied by a change in the remaining amide I contribution (i.e., a change in the overall C=O stretching) and a broadening in the contribution of water outside the network. Regarding instead the native phase, it is observable a marked change in both the C–N stretching and N–H bending modes on crossing T_L ; at the same time changes in the water contributions appear not significant. On these bases we consider a more care analysis of these amide II and water contributions in the large T -interval studied.

III. RESULTS

We examine the bending vibrational mode of water and the amide I and amide II modes of the lysozyme and demonstrate that the HBs in water molecules—with the carbonyl oxygen (C=O) and an amide N–H molecular groups of the protein peptides—trigger the biomolecular “dynamic” transition. The most stable water-protein configuration has two HBs, a water proton donor bond to the carbonyl oxygen and an amide N–H proton donor bond to the water oxygen.^{44,45} The role of the HBs in water plays in protein folding, in protein-protein binding, and in molecular recognition is also well-known because of such thermodynamic behavior as heat capacity effects.⁴⁶ In short, water acts as a HB “glue” between the carbonylic and amidic groups of a protein.⁴⁷

HBs govern the secondary structure in proteins and the specificity of folding³⁸ that affects IR absorption lines in both the frequency and the extinction coefficient because the normal mode force constant is modified.³ An example of this are the amide groups, whose position helps to identify the α and β helices in proteins. The secondary structure assignment procedures based on IR generally use a single frequency as “ α -helical” and the measured spectra differ significantly between solvent (water) exposed and solvent-inaccessible α helices.⁴⁸ In order to study the role of water at the protein dynamical transition ($T_L \approx 225$ K) at a molecular level and inside the native state, we focus on the temperature evolution of the obtained spectra for hydrated lysozyme in the range $180 < T < 350$ K. We observe that the protein-water vibrational dynamics change significantly (a change reflected in the amide I and II bands) at the FSDC and at the irreversible protein unfolding ($T_D \approx 345$ K). In order to clarify how HBs drive the properties of protein, we have considered in detail these dynamic contributions and those of the protein hydration water as a function of T .

We use neutron and NMR spectroscopy to obtain the dynamic protein transition and the dynamic crossover in water. The upper panel of Fig. 3 shows the MSD averaged over all the hydrogen atoms, $\langle X^2 \rangle$, extracted from the Debye-Waller factor, measured using elastic neutron scattering, as a function of T for hydrated lysozyme with H_2O (circles, upper curve) and D_2O at $h = 0.3$.²⁰ The inset shows the inverse of

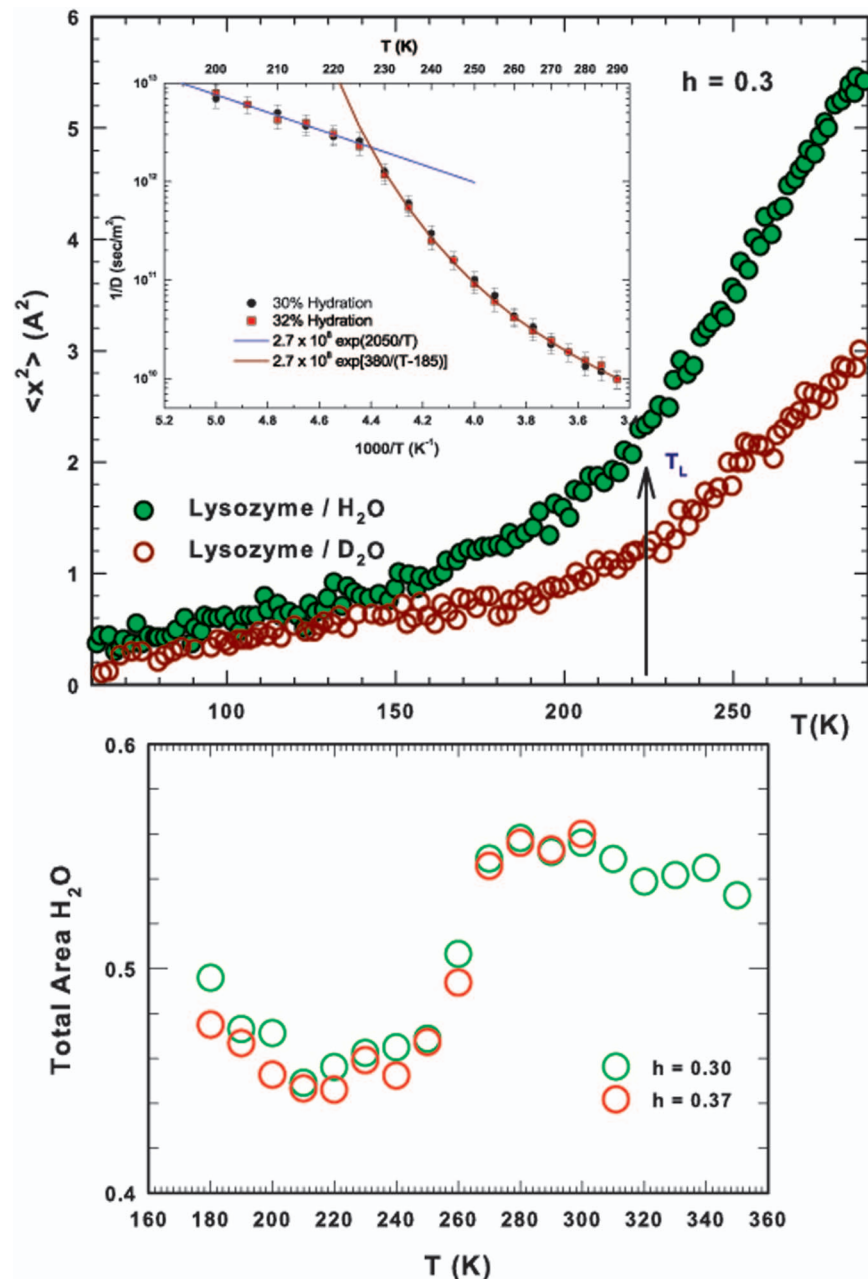


FIG. 3. Evidence for the protein dynamic transition. (Top panel) The mean-squared atomic displacement MSD averaged over all the hydrogen atoms, $\langle x^2 \rangle$, as a function of temperature for the H_2O and D_2O hydrated lysozyme samples at the hydration level $h = 0.30$.²⁰ The arrow indicates the crossover temperature T_C . In the inset is reported the behavior of the protein water self-diffusion coefficient $D(T)$, at the same hydration, that shows the strong-fragile crossover at $T_L \approx T_C$.⁴⁹ (Bottom panel) The spectral area, relative to the total FTIR measured area, of the water bending components for $h = 0.3$ and 0.37 .

the water self-diffusion coefficient D , obtained using NMR spectroscopy.⁴⁹ The data of the Lyso/ D_2O are used to evaluate the MSD of the protein hydrogen atoms. From these two curves we conclude that the FSDC temperature of the hydration water and the dynamic transition temperature of the protein are approximately the same (within the error bars of the kink positions).

The MSD behavior indicates the “softness” of the protein. Protein flexibility, essential to their enzymatic catalysis and their other biological functions, results from conformational disorder in the protein. In dynamic terms it is the response of the protein to applied forces that maintains its biological structure and, in the case of macromolecules, gov-

erns atomic motions.³² Under ambient conditions biopolymers are “soft.” Their “softness” can be evaluated from the displacement X of a given atom in response to a given applied force F in terms of Hooke’s law. This is done by assuming that the atom is bonded to the protein by a spring with a spring constant K , i.e., $X = F/K$. Thus for a given F , the smaller the spring constant K , the larger the displacement X and the softer the biological material. Figure 3 (top panel) shows that the protein crossover is related to a change in protein flexibility from a nearly rigid state to a flexible state when T is increased above T_L . This is supported by the behavior of the self-diffusion coefficient $D(T)$ when there is a FSDC at T_L [see inset of Fig. 3 (top panel)]. Both of these

quantities are strongly connected, in pure Brownian motion, $\langle X(T)^2 \rangle = 2Dt$, and in motions governed by clustering processes, $\langle X(T)^2 \rangle \sim Dt^\gamma$, where the exponent γ is related to the cluster properties.⁵⁰ Both of these results confirm that, through coincident changes in protein softness and its energetic configurations, the behavior of protein water is linked to the dynamics and behavior of the biomolecule. When we increase T , FSDC reflects a change in its energy landscape from a hopping over barriers of uniform height (the strong Arrhenius) to a multi-relaxation due to local and rapid intrabasin dynamics (the fragile Super-Arrhenius). Our goal here is to clarify the molecular origin, the mechanisms, and the effects of these correlations between water and protein molecules.

The study of water and water solutions has traditionally focused on molecular stretching modes that are easily accessible using standard Raman and infrared spectroscopic techniques because of their high absorption cross-sections and frequencies. The relaxation of vibrational excitations in water reflects its physical properties.⁴² The bending modes also exhibit analogous features because they are sensitive to HB frequency, HB strength, and water molecules connectivity.

Bending mode relaxation differs from stretching because it occurs through intermolecular interactions and consequent energy transfers (whereas the stretching is essentially an intramolecular mode). These couplings occur in pure systems and in solutions with the difference that in the second case these intermolecular interactions involve an energy transfer between solute and solvent (i.e., protein and water).⁵¹

The vibrational bending modes of pure bulk water and some of the peptide fall, as illustrated in Sec. II (Figure 1), in the same spectral region ($1300 < \nu < 1800 \text{ cm}^{-1}$). Water has essentially two bending modes—one at $\sim 1560 \text{ cm}^{-1}$ caused by molecules clustered in the network (i.e., only the four-bonded or LDL), and one at $\sim 1640 \text{ cm}^{-1}$ that is sharper and represents the remaining, non-clustered free network molecules (HDL).⁴² Smaller is the line-width, more homogeneous is the molecular phase. Whereas those of the peptide are the amide I, II, and III, used to assign proteins secondary structure.⁴¹

The amide I absorption band is primarily determined by the backbone conformation and is mainly associated with the C=O stretching vibration related to the protein backbone. Contribute to this band: the α -helix ($1650\text{--}1657 \text{ cm}^{-1}$), the antiparallel β -sheets (two contributions in the ranges $1612\text{--}1640 \text{ cm}^{-1}$ and $1680\text{--}1689 \text{ cm}^{-1}$) and the random coil near 1680 cm^{-1} . The amide II results essentially from the N–H bending vibration and from the C–N stretching vibration, respectively, at 1540 and 1520 cm^{-1} . This latter stretching, conformationally sensitive, is related with the antiparallel β -sheet structure of peptides and proteins.

Here, we focus our interest on the two water bending components, the amide I and the amide II. We study the spectra in the native phase, before and after the FSDC, exhibiting different absorbance behaviors such as marked changes in both the C–N stretching and N–H bending modes when T_L is crossed. Differences are also observed between the native and denatured protein states: in the native one the amide I band is fairly asymmetric and has a peak maximum around 1650 cm^{-1} corresponding to alpha-helical structure, whereas

the denatured proteins show an additional maximum between 1620 and 1650 cm^{-1} , indicative of the predominance of an antiparallel intermolecular β -sheet and the onset of an un-ordered aggregation process.⁴³ The measured spectra are customary analyzed, see Sec. II, as a spectral deconvolution of Gaussian band shapes by an iterative curve fitting procedure obtaining their integrated areas, the frequency and the FWHM. We stress that for the working spectral resolution the frequency variation with the temperature was not taken into account.

Figure 3 (bottom panel) shows the contrast between the spectral area and the total FTIR measured area of the water-bending components for $h = 0.3$ and 0.37 . We see an emerging behavior similar to that of the water density ρ measured as a function of T in confined water characterized by a maximum at 277 K and a minimum at approximately 200 K .⁵² This is not surprising because a spectral component area (in scattering) is proportional to the number of molecules from which it originates. Figure 3 (top panel) shows this result together with the behaviors of the MSD and $1/D$ as a function of T . The density maximum and density minimum of water in the supercooled regime have been associated with liquid polymorphism and hence to the dominance of the HDL over the LDL for the maximum and the opposite for the minimum. The LDL characterizes the HB network dominating the low- T regime (it is more rigid), and the HDL characterizes the high- T liquid phase (it is softer) in which the dominance of the partially-bonded and free water molecules increases with T . This temperature evolution of the MSD of all the hydrogen atoms in the protein and in the internal and hydration protein water was also proposed as an explanation for the dynamic crossover observed in such transport parameters as D .⁷

Figure 4 shows the FWHM of the water bending component (upper panel) and of the amide II component (lower panel). It also shows bulk water and nanotube-confined water data. Note that bulk and confined water have similar FWHM values in the two HB components, but that the protein water as a function of T exhibits completely different behavior. The protein water FWHM of the two components is nearly constant as T is increased from the deep supercooled phase to the stable liquid phase (but in confined water they progressively narrow); a situation suggesting that the corresponding dynamics are strongly localized, but that the same spectral quantity in nanotube-confined water indicates a change from a broad to a narrow energetic configuration. The two systems differ in that, unlike nanotube-confined water, protein water cannot change its dynamic configuration. As mentioned above, because intermolecular bending is a form of energy transfer between solute and solvent, in bulk and nanotube water the interactions are among different water molecules and in hydrophilic groups between water and protein.

The behavior of amide II, with the contribution of N–H bending and C–N stretching, is dramatically different. Their FWHM shows a protein “dynamic” transition temperature of the FSDC of water that marks the border between two differing dynamic regions. When $T < T_C$, the energetic configuration of the two modes differ greatly, the C–N stretching has a FWHM value of $\sim 50 \text{ cm}^{-1}$, the N–H bending is narrower $\sim 20 \text{ cm}^{-1}$, and these values are T -independent in the

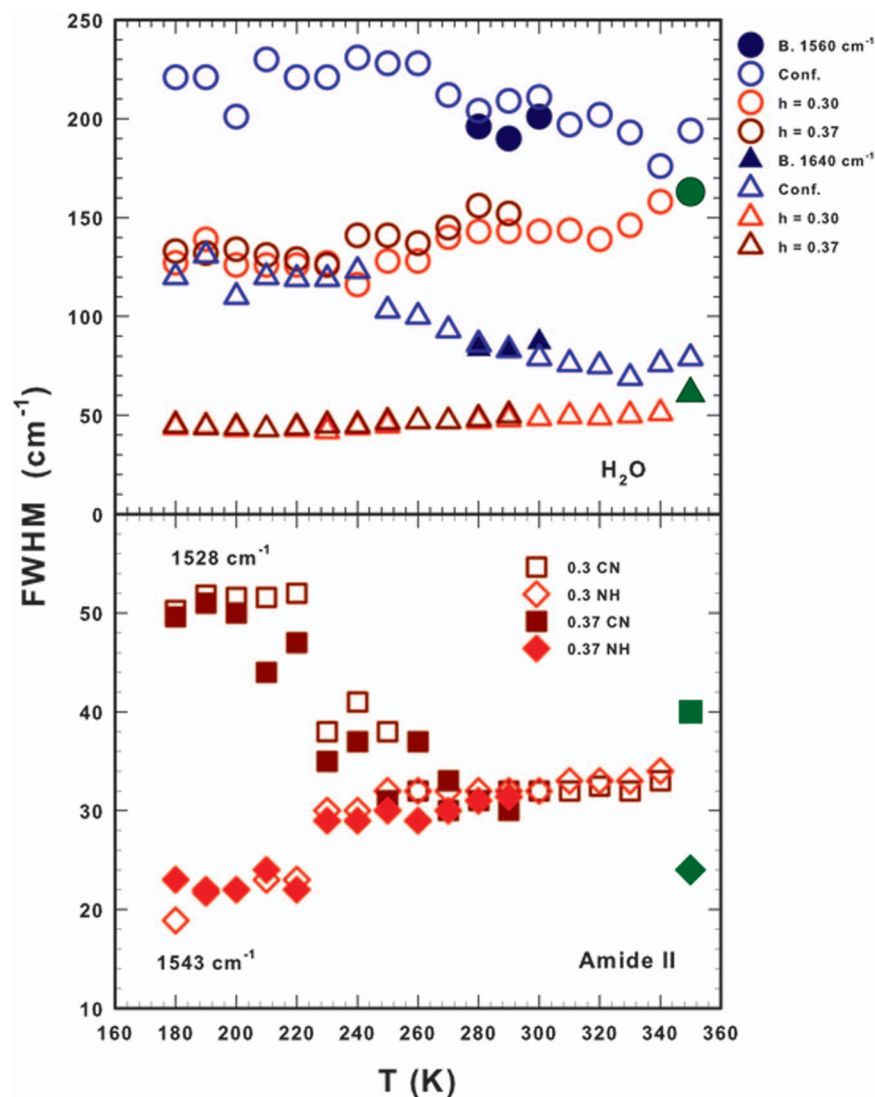


FIG. 4. The temperature behaviors of the extracted FWHM of the water bending (top panel) and of the amide II components (bottom panel) for hydrated lysozyme samples ($h = 0.3$ and 0.37). Data measured in bulk and water confined in nanotubes are also reported. Circles regard the contribution of fully bonded molecules belonging to the HB tetrahedral network (or LDL at ~ 1560 cm^{-1}) whereas triangles represent the remaining part (HDL). For the amide II component the contributions of the N–H bending and C–N stretching are reported. These latter data give evidence of a dramatic change just at T_C . Error bars are comparable to the data symbol size.

range 180–220 K. When T is increased the FWHM of the N–H bending undergoes a sharp transition near T_C to a value of ~ 30 cm^{-1} , and the corresponding quantity of C–N stretching modes decreases to the same value in a larger T interval. When $T > 270$ K, the two modes have approximately the same FWHM that increases slowly with T until reaching the protein unfolding temperature.

Figure 5 shows the temperature evolution of the relative area between the two components of the bending water (top panel) and the area of the amide II contributions (bottom panel) with respect to the total measured area. In both panels we see a change at approximately the protein dynamical transition (T_C or T_L). All the quantities appear T -independent in the protein harmonic solid regime 180–220 K, but when $T > T_L$ the quantities change as T increases. More precisely, the area of N–H bending in the amide II increases with T , as does the bending of the water molecules outside the network. The opposite behavior is found in the C–N stretching area

and in the fully tetrabonded water, which resemble the behavior observed in the corresponding FWHMs. This is related to system dynamics in that water behavior in the harmonic stable regime ($T < T_L$) is strongly influenced by its low-density fully-developed HB network, i.e., by the two HBs and properties of the protein peptides.

IV. DISCUSSION

Although the NH–O HB is influenced by N–H bending, the strongest influence comes from the proton donors (C=O–HO bonds) which are connected to the C–N stretching mode of the amide II. Water accessibility affects IR spectra⁵³ and the HBs modify the normal-mode force constant.³ We also observe that the HBs produced by the hydrophilic carbonyl and N–H groups in external water distorts protein structure⁵⁴ and dynamics.⁵³ The crystal structure can be hydrated, either externally by a water molecule HB to the C=O

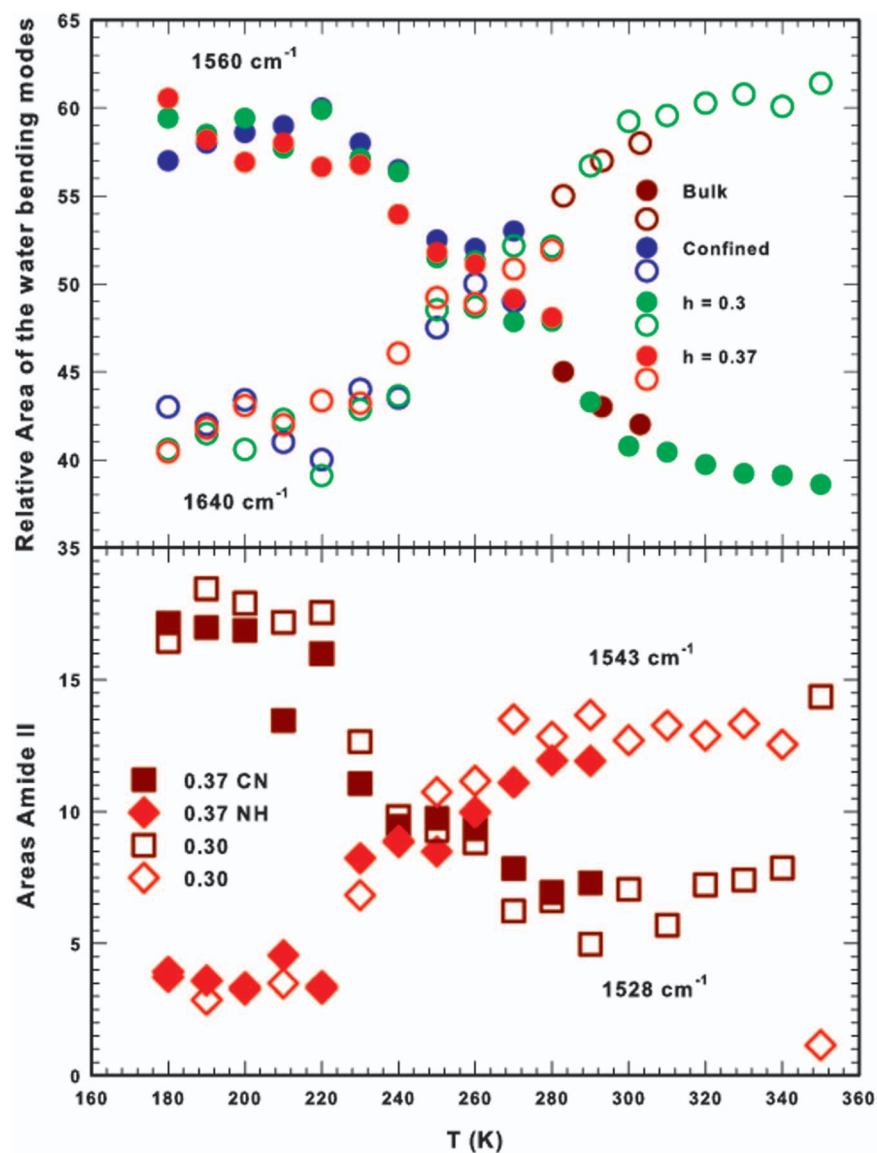


FIG. 5. The temperature evolution of the relative area between the two components (network molecules and outside) of the bending water (top panel). The relative areas, with respect to the total spectral area, of the amide II contributions (bottom panel). Error bars are comparable to the data symbol size.

backbone, or internally by forming a HB bridge between this group and the amide group. Figure 5 shows this by showing the change in molecular behavior activity in the T -range from the harmonic supercooled phase to the irreversible unfolding phase. Figure 5 also shows that for $T < T_L$ the C–N stretching dominates over the other and that the relative ratio is approximately 6:1. When $T > T_L$ (and for $T > T_M$) the behavior is the opposite with an areas ratio approximately 1:2. When the protein denatures, this ratio reverses again at 15:1 or even greater, and there is an onset of a large antiparallel intermolecular β -sheet in the amide I band dominated by C=O stretching and protein aggregation.⁴³ Our data also show that protein properties and thermal stability in the anharmonic regime above the FSDC up to the denaturation, are regulated by an equilibration of the HBs connecting water and peptides involving both internal and hydration species. This is confirmed by the T -behavior of the corresponding FWHMs (see Fig. 4). On the other hand, below T_L the C–N stretching has a larger FWHM

value, with respect to the N–H bending, indicating a different energetic configuration. Very similar curves to those of Fig. 5 have been obtained in a MD simulation for the inherent structures.¹³

Finally, the bending contribution of water inside (LDL) and outside the network (HDL) extracts an enthalpy value H that corresponds to the HB formation process by means of the van't Hoff expression (relating the T -dependence of an equilibrium constant K to the H change as $d\ln K/d(1/T) = -\Delta H/R$). Figure 6 shows a log-linear plot of the ratio I_{NET}/I_{NC} of the integrated areas of the fully tetrabonded molecules (1560 cm^{-1}) and the molecules outside the network and not clustered (1640 cm^{-1}) versus $1/T$. In order to clarify some aspects of the role of water in protein activity, we assume that the ratio I_{NET}/I_{NC} is directly related to K and, from $\ln(I_{NET}/I_{NC}) = -\Delta H/RT$, we obtain the HB enthalpy variation in the large T interval studied here. Figure 6 shows the results, which confirm that two different regimes can be seen

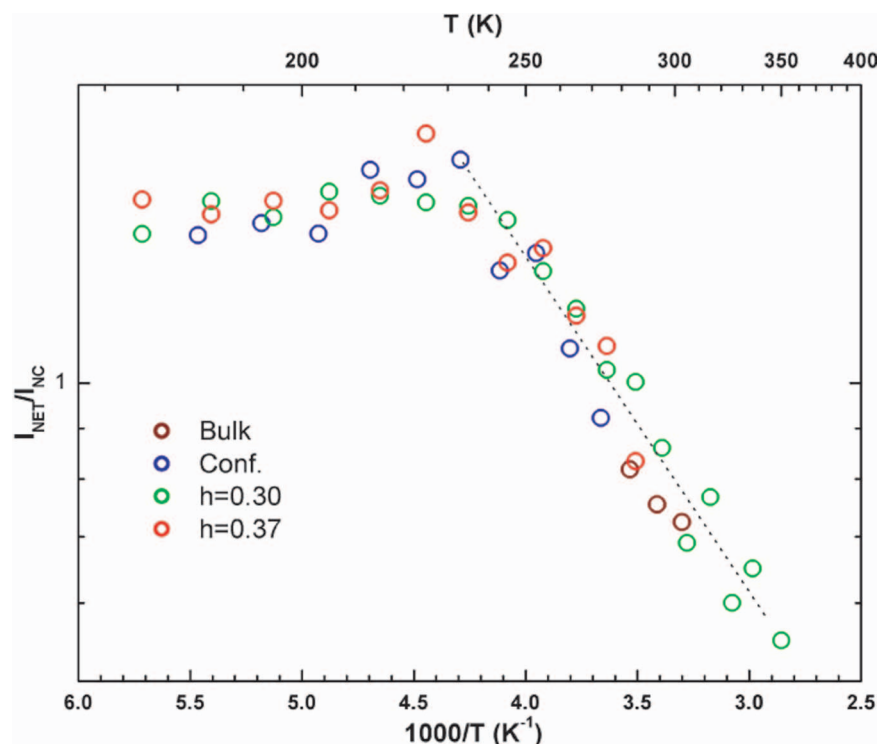


FIG. 6. The ratio I_{NET}/I_{NC} on a logarithmic scale versus $1000/T$. The dashed line through the data represents the linear least-squares fit. Error bars are comparable to the data symbol size.

immediately above and below the water FSDC (the protein dynamic transition). Below the crossover the ratio value between the areas remains approximately constant as T decreases, indicating that in the protein harmonic solid-like state the majority of water molecules are either linked to the tetra-bonded water cluster (the network or LDL phase) or linked to the protein by means of C=O–HO and NH–O bonds. The probability of forming or breaking a HB is small and hopping between clusters is the only water motion (see the inset of Fig. 3). When T is increased above T_L , everything changes. The HBs in the anharmonic protein liquid phase can be formed and broken and the corresponding probability evolves with T according to the van't Hoff equation. When $T > T_L$, the data reported in Fig. 6 can be fit to obtain the corresponding ΔH up to the irreversible denaturation (the dashed line through the data represents the linear least-squares fit). The measured enthalpy change of the water HB is ~ 2.3 kcal/mol (typical of HBs). In conclusion, this analysis indicates that above the water FSDC (and hence the protein dynamical crossover) all protein water (internal and of hydration) recovers the HB dynamics (rupture and formation) that had been frozen in the harmonic “glass” state, thus allowing “activity” up to the irreversible denaturation.

ACKNOWLEDGMENTS

The research at MIT was supported by a grant from Basic Energy Sciences Division of US DOE DE-FG02-90ER45429. H.E.S. thanks the NSF Chemistry Division for support (Grant No. CHE-1213217).

- ¹P. G. Debenedetti and H. E. Stanley, “Supercooled and glassy water,” *Phys. Today* **56**, 40–46 (2003).
- ²Y. Levy and J. N. Onuchic, *Annu. Rev. Biophys. Biomol. Struct.* **35**, 389–415 (2006).
- ³G. A. Jeffrey and W. Saenger, *Hydrogen Bonding in Biological Structures* (Springer-Verlag, Berlin, 1991).
- ⁴S. H. Chen *et al.*, *Proc. Natl. Acad. Sci. U.S.A.* **103**, 12974–12978 (2006).
- ⁵F. Mallamace *et al.*, *Proc. Natl. Acad. Sci. U.S.A.* **104**, 424–428 (2007).
- ⁶L. Xu *et al.*, *Nat. Phys.* **5**, 565–569 (2009).
- ⁷F. Mallamace *et al.*, *Proc. Natl. Acad. Sci. U.S.A.* **107**, 22457–22462 (2010).
- ⁸S. Yip and M. P. Short, *Nat. Mater.* **12**, 774–777 (2013).
- ⁹F. Mallamace, C. Corsaro, H. E. Stanley, and S.-H. Chen, *Eur. Phys. J. E* **34**, 94 (2011).
- ¹⁰J. C. Martinez-Garcia, J. Martinez-Garcia, S. J. Rzoska, and J. Hulliger, *J. Chem. Phys.* **137**, 064501 (2012).
- ¹¹T. Hecksher, A. I. Nielsen, N. Boye Olsen, and J. C. Dyre, *Nat. Phys.* **4**, 737–741 (2008).
- ¹²J. C. Mauro, Y. Yue, A. J. Ellison, P. K. Gupta, and D. C. Allan, *Proc. Natl. Acad. Sci. U.S.A.* **106**, 19780–19784 (2009).
- ¹³K. T. Wikfeldt, A. Nilsson, and L. G. M. Pettersson, *Phys. Chem. Chem. Phys.* **13**, 19918–19924 (2011).
- ¹⁴P. Kumar, K. T. Wikfeldt, D. Schlesinger, L. G. M. Pettersson, and H. E. Stanley, *Sci. Rep.* **3**, 1980 (2013).
- ¹⁵S.-H. Chen *et al.*, *J. Phys.: Condens. Matter* **21**, 504102 (2009).
- ¹⁶A. Paciaroni, A. R. Bizzarri, and S. Cannistaro, *Phys. Rev. E* **60**, R2476(R) (1999).
- ¹⁷G. Schiro, F. Natali, and A. Cupane, *Phys. Rev. Lett.* **109**, 128102 (2012).
- ¹⁸F. H. Stillinger, *Science* **267**, 1935–1939 (1995).
- ¹⁹S. H. Chen *et al.*, *Proc. Natl. Acad. Sci. U.S.A.* **103**, 9012–9016 (2006).
- ²⁰X. Q. Chu *et al.*, *J. Phys. Chem. B* **113**, 5001–5006 (2009).
- ²¹G. Caliskan *et al.*, *J. Am. Chem. Soc.* **128**, 32–33 (2006).
- ²²M. Lagi *et al.*, *J. Phys. Chem. B* **112**, 1571–1575 (2008).
- ²³M. F. Fomina, G. Schiro, and A. Cupane, *Biophys. Chem.* **185**, 25–31 (2014).
- ²⁴K. L. Ngai, S. Capaccioli, and A. Paciaroni, *Chem. Phys.* **424**, 37–44 (2013).

- ²⁵G. Schirò, V. Vetri, C. B. Andersen, F. Natali, M. M. Koza, M. Leone, and A. Cupane, *J. Phys. Chem. B* **118**, 2913–2923 (2014).
- ²⁶W. Doster, S. Busch, A. M. Gaspar, M.-S. Appavou, J. Wuttke, and H. Scheer, *Phys. Rev. Lett.* **104**, 098101 (2010).
- ²⁷M. Rosenstihl and M. Vogel, *J. Chem. Phys.* **135**, 164503 (2011).
- ²⁸F. H. Stillinger, *J. Chem. Phys.* **88**, 7818–7825 (1988).
- ²⁹H. Frauenfelder, G. A. Petsko, and D. Tsernoglou, *Nature* **280**, 558–563 (1979).
- ³⁰I. E. T. Iben *et al.*, *Phys. Rev. Lett.* **62**, 1916–1919 (1989).
- ³¹F. Parak and E. W. Knapp, *Proc. Natl. Acad. Sci. U.S.A.* **81**, 7088–7092 (1984).
- ³²G. Zaccai, “How soft is a protein?” *Science* **288**, 1604–1607 (2000).
- ³³B. F. Rasmussen, A. M. Stock, D. Ringe, and G. A. Petsko, *Nature* **357**, 423–424 (1992).
- ³⁴J. A. Rupley and G. Careri, “Protein hydration and function,” *Adv. Protein Chem.* **41**, 37–172 (1991).
- ³⁵W. Doster, S. Cusack, and W. Petry, *Nature* **337**, 754–756 (1989).
- ³⁶M. Ferrand, A. J. Dianoux, W. Petry, and G. Zaccai, *Proc. Natl. Acad. Sci. U.S.A.* **90**, 9668–9672 (1993).
- ³⁷G. Careri, *Prog. Biophys. Mol. Biol.* **70**, 223–249 (1998).
- ³⁸L. Pauling, R. B. Corey, and H. R. Branson, *Proc. Natl. Acad. Sci. U.S.A.* **37**, 205–211 (1951).
- ³⁹D. Russo, G. L. Hura, and J. R. D. Copley, *Phys. Rev. E* **75**, 040902 (2007).
- ⁴⁰M. Tarek and D. J. Tobias, *Phys. Rev. Lett.* **88**, 138101 (2002).
- ⁴¹J. T. Pelton and L. R. McLean, *Anal. Biochem.* **277**, 167–176 (2000).
- ⁴²G. E. Walrafen, M. R. Fisher, M. S. Hokomabadi, and W. H. Yang, *J. Chem. Phys.* **85**, 6970–6982 (1986).
- ⁴³S. Adams, A. M. Higgins, and R. A. L. Jones, *Langmuir* **18**, 4854–4861 (2002).
- ⁴⁴E. S. Eberhardt and R. T. Raines, *J. Am. Chem. Soc.* **116**, 2149–2150 (1994).
- ⁴⁵S. T. R. Walsh *et al.*, *Protein Sci.* **12**, 520–531 (2003).
- ⁴⁶A. Cooper, *Biophys. Chem.* **115**, 89–97 (2005).
- ⁴⁷M. Sundaralingam and Y. C. Serkharudu, *Science* **244**, 1333–1337 (1989).
- ⁴⁸R. Gilmanshin, S. Williams, R. H. Callender, W. H. Woodruff, and R. B. Dyer, *Proc. Natl. Acad. Sci. U.S.A.* **94**, 3709–3713 (1997).
- ⁴⁹F. Mallamace *et al.*, *J. Phys. Chem. B* **114**, 1870–1878 (2010).
- ⁵⁰F. Mallamace *et al.*, *J. Chem. Phys.* **139**, 214502 (2013).
- ⁵¹O. F. A. Larsen and S. Woutersen, *J. Chem. Phys.* **121**, 12143–12145 (2004).
- ⁵²F. Mallamace *et al.*, *Proc. Natl. Acad. Sci. U.S.A.* **104**, 18387–18391 (2007).
- ⁵³J. D. Eaves, C. J. Fecko, A. L. Stevens, P. Peng, and A. Tokmakoff, *Chem. Phys. Lett.* **376**, 20–25 (2003).
- ⁵⁴T. Blundell, D. Barlow, N. Borkakoti, and J. Thornton, *Nature* **306**, 281–283 (1983).